Protoplasma (2022) 259:937–948
https://doi.org/10.1007/s00709-021-01712-3

ORIGINAL ARTICLE

Biochemical and morphological characterization of freshwater microalga *Tetradesmus obliquus* (Chlorophyta: Chlorophyceae)

Cristiane do Carmo Cesário[1] · Jimmy Soares[2] · Jamile Fernanda Silva Cossolin[3] · Allan Victor Martins Almeida[4] · Jose Jovanny Bermudez Sierra[5] · Mauricio de Oliveira Leite[2] · Maria Clara Nunes[6] · José Eduardo Serrão[3] · Marcio Arêdes Martins[2] · Jane Selia dos Reis Coimbra[1]

Received: 15 March 2021 / Accepted: 29 September 2021 / Published online: 13 October 2021

Abstract

Tetradesmus is a microalgal genus with biotechnological potential due to its rapid production of biomass, which is plenty in proteins, carbohydrates, lipids, and bioactives. However, its morphology and physiology need to be determined to guide better research to optimize the species cultivation and biocompounds processing. Thus, this study describes the biochemistry and morphology of the strain *Tetradesmus obliquus* BR003, isolated from a sample of freshwater reservoirs in a Brazilian municipality. In the *T. obliquus* BR003 dry biomass, we identified 61.6% unsaturated fatty acids, and 3.4% saturated fatty acids. Regarding other compounds, 28.50 ± 1.47 g soluble proteins/100 g, 0.14 ± 0.009 g carotenoids/100 g, 0.76 ± 0.013 g chlorophyll a/100 g, and 0.42 ± 0.015 g chlorophyll b/100 g with a chlorophyll a/b ratio of 1.8 were detected. The main chemical elements found were S, Mg, and P. The cells of BR003 were elliptically curved at the ends and without appendages. Histochemical tests showed carbohydrates distributed in the cytoplasm and pyrenoids, some lipid droplets, and proteins. The cytoplasm is rich in vacuoles, rough endoplasmic reticulum, mitochondria, and chloroplasts. The nucleus has a predominance of decondensed chromatin, and the cell wall has three layers. Chloroplasts have many starch granules and may be associated with a spherical central pyrenoid. To the best of our knowledge, this was the first biochemical description combined with ultrastructural morphological characterization of the strain *T. obliquus* BR003, grown under standard conditions, to demonstrate specific characteristics of the species.

Keywords *Scenedesmus obliquus* · Green algae · Microscopy · Histochemistry

Handling Editor: Andreas Holzinger

✉ Cristiane do Carmo Cesário
cristiane.cesario@ufv.br

✉ José Eduardo Serrão
jeserrao@ufv.br

[1] Department of Food Technology, Universidade Federal de Viçosa, Viçosa, Brazil

[2] Department of Agricultural Engineering, Universidade Federal de Viçosa, Viçosa, Brazil

[3] Department of General Biology, Universidade Federal de Viçosa, Viçosa, Brazil

[4] Department of Plant Physiology, Universidade Federal de Viçosa, Viçosa, Brazil

[5] Graduate Program in Biotechnology (RENORBIO), Universidade Federal do Ceará, Fortaleza, Brazil

[6] Department of Veterinary Medicine, Universidade Federal de Viçosa, Viçosa, Brazil

Introduction

Microalgae use inorganic and organic components to produce and accumulate biocompounds that can be used in various agro-industrial segments (Rizwan et al. 2018). They are promising for agriculture since it is possible to produce them using anthropogenic emissions such as carbon dioxide, agro-industrial effluents, and wastewater for agriculture (Falconí et al. 2021; Rocha et al. 2019). Microalgae have been used in animal and human food (Amorim et al. 2020a; Hossain et al. 2017and in the production of bread (Uribe-Wandurraga et al. 2019; García-Segovia et al. 2017), yogurt (Barkallah et al. 2017), and pasta (Fradique et al. 2010).

Microalgae can accumulate high levels of essential fatty acids that are relevant to nutrition, like polyunsaturated fatty acids ω-3 (eicosapentaenoic and docosahexaenoic acids), ω-6 (arachidonic and linoleic acids), and ω-9 (oleic and nervonic acids) (Guedes et al. 2011; Rubio-Rodríguez

et al. 2010). Additionally, microalgae have high levels of pigments, including chlorophylls, xanthophylls, and carotenes used as natural food dyes (Bermejo et al. 2007). Some microalgae can also accumulate high levels of reserve carbohydrates and lipids (Takeshita et al. 2014).

Detailed knowledge of the accumulation phenomena of biochemical components in specific strains or genera of microalgae is scarce, mainly due to the diversity of these photosynthesizing microorganisms. Knowledge of a microalgae strain's cellular structure can help develop methods for monitoring productivity in commercial farms and more efficient biomass biorefining processes (Bensalem et al. 2020).

Among the various genera of microalgae, *Tetradesmus* (Chlorophyceae) (Wynne and Hallan, 2015), formerly *Scenedesmus*, present commercial use potential (Breuer et al. 2014; Dahlin et al. 2018). *Tetradesmus* are characterized by a high degree of phenotypic plasticity, with great differentiation between strains (Lürling 2003). It can withstand adverse conditions such as temperature variations, nutritional stress, and predation (Lürling 2003; Rocha et al. 2019; Covell et al. 2019).

Tetradesmus obliquus BR003, a Chlorophyte green algae of tropical origin (Rocha et al. 2017), has been broadly characterized by its metabolic diversity under different growing conditions. Amorin et al. (2020) cultivated BR003 in a pond with an adductor canal for 15 days to optimize the extraction of proteins and lipids and obtained biomass with just over 33% and 5% of soluble proteins and lipids, respectively. Vieira et al. (2020), under similar conditions, obtained approximately 32% of proteins, a little more than 10% of lipids, 0.6% of total chlorophyll, and 0.16% of carotenoids. Covell et al. (2020) evaluated alternative growth media for BR003 indoors and outdoors. After 10 days of culture, they found approximately 16% of lipids, 45% of proteins, 35 µg/mg of total chlorophyll, and 9 µg/mg of carotenoids. Silva et al. (2020) studied the food safety of *T. obliquus* biomass in an animal model. The biomass cultivated for 12 days contained a significant amount of protein (40.42%), insoluble fiber (16.23%), soluble fiber (3.14%), phenolic compounds (1.96%), carotenoids (1.10%), oleic C18:1 (1.38%), linoleic C18:2 (0.95%), and linolenic acids C18:3 (0.28%). Rocha et al. (2019) described the greater accumulation of esterifiable neutral lipids (mono-, di-, and tri-glycerols) and free fatty acids for BR003 under specific cultivation conditions. Rocha et al. (2017) reported higher productivity for BR003 compared to other strains. Despite the suitability of *T. obliquus* BR003 for biotechnological use (Amorim et al. 2021; Vieira et al. 2021), its morphology has not yet been characterized. The species identification was performed only by the molecular phylogeny of the 18S ribosomal RNA sequences and the ITS2 internal transcribed spacer region (Rocha et al. 2017). These authors found 18% of lipids, with C16, C18:1, and C18:2 being the most expressive fatty acids. Therefore, the present study describes the biochemical composition of reserve compounds (lipids, chlorophyll, carotenoids, and proteins) in combination with the cytology and morphology of *T. obliquus* BR003. These types of information can contribute to research lines that optimize pre-treatment techniques to obtain algal biocompounds.

Material and methods

Production and cultivation of *Tetradesmus obliquus* BR003

The strain *T. obliquus* BR003 was previously isolated from a sample of freshwater reservoirs on the *campus* of the Universidade Federal de Viçosa (UFV) (Rocha et al. 2017) and kept in the Collection of Cyanobacteria and Microalgae (CCM-UFV) of the Laboratory of Phycology and Molecular Biology of the Department of Plant Biology (UFV), Viçosa, Minas Gerais, Brazil.

The biomass of *T. obliquus* BR003 was produced as described by Covell et al. (2020), using BG11 culture medium (Rippka et al. 1979) under conditions of pH 7.0, 24 ± 1 °C, 70 µmol/m^2/s light intensity, 16:8 h (light:dark) photoperiod, and 100 rpm of orbital shaking. After 68 h, cells of *T. obliquus* BR003 in the exponential growth phase were collected by centrifugation at 4000 g for 5 min at 4 °C. The precipitate was resuspended in deionized water following further centrifugation and repeated three times. One part of the biomass was frozen at − 20 °C, lyophilized (Terroni, LS 30,000, Brazil) at − 48 °C for 24 h, and another part was diluted in a solution suitable for each evaluation.

Determination of the fatty acid profile

The determination of the fatty acid profile of *T. obliquus* BR003 was performed from the transesterification of lipids extracted with a mixture of chloroform and methanol (2:1). The transesterification reaction was performed using an 8% solution (v/v) of HCl in methanol at 100 °C for 1 h (Ichihara and Fukubayashi 2010). Methyl esters were recovered with hexane, identified, and quantified in a gas chromatograph coupled to a flame ionization detector (GC-2010, Shimadzu, Japan) equipped with a 100 m × 0.25 mm capillary column (SP-2560, Sigma-Aldrich, USA). The analysis was performed by direct injection of 1 µL of the sample. Helium was used as a carrier gas, maintaining a constant flow rate of 40 mL/min and pressure of 363 kPa. The separation of methyl esters from fatty acids occurred using a linear heating ramp from 60 to 330 °C at a heating rate of 20 °C/min. The

identification of the peaks was confirmed by comparison with a mixture of fatty acid methyl ester patterns (Supelco 37 FAME mix, Sigma-Aldrich, United States).

Total chlorophyll and carotenoids

A 2 mL volume of methanol with 99.9% purity was added in 2 mg of the lyophilized biomass. The extract was homogenized, incubated in the dark for 24 h at 45 ºC, and then centrifugated (Eppendorf, 5430, Germany) at 10,000 *g* for 10 min. The supernatant was separated, and the absorbance was read in a spectrophotometer (Multskan GO, Thermo Scientific, Germany) at 470, 652, and 665 nm. The experiments were performed in triplicate. The pigment content was determined using Eqs. 1, 2, 3, as proposed by Lichtenthaler (1987):

$$Clo(\mu g/mL) = 16.72A_{665} - 9.16A_{652} \quad (1)$$

$$Clb(\mu g/mL) = 34.09A_{652} - 15.28A_{665} \quad (2)$$

$$Car(\mu g/mL) = 1000A_{470} - 1.63Cla - 104.96Clb \quad (3)$$

where A is the absorbance at the selected wavelengths, Cla and Clb represent chlorophyll a and chlorophyll b, respectively, and Car refers to carotenoid.

Proteins

Extraction of total hydrosoluble proteins was carried out according to Meijer and Wijffels (1998), and quantification was performed by Lowry's method (Lowry et al. 1951), as described by Rocha (2019). Bovine serum albumin (fraction V powder, Sigma-Aldrich, USA) was used to prepare the standard curve. The experiments were performed in triplicate.

Light microscopy

T. obliquus BR003 cells were fixed in Zamboni solution (Castro et al. 2020) for 24 h. The fixed cells were dehydrated using a gradient of aqueous ethanol solutions (70%, 80%, 90%, and 95%, v/v) and soaked in historesin Leica. Two-micrometer-thick sections were stained with hematoxylin and eosin and analyzed under a light microscope (Bx60, Olympus, Japan).

Histochemistry

Another set of slices was submitted to the Schiff periodic acid (PAS) test to detect neutral carbohydrates and glycoconjugates, Nile blue to detect acidic and neutral lipids, and mercury-bromophenol to detect total proteins (Pearse, 1953).

Confocal microscopy

Three samples of viable cultures of *T. obliquus* BR003 cells were washed twice with phosphate-buffered saline (PBS) (0.1 M and pH 7.2), buffer A, and centrifugated (Eppendorf, 5430, Germany) at 4.000 *g* for 5 min. The cells were then incubated in a mixture of 20 µg/mL propidium iodide (for DNA visualization) and 2 µg/mL fluorescein isothiocyanate in buffer A (for protein visualization) for 15 min each in the dark (Ribeiro et al. 2018). The samples were washed with buffer A and examined under a confocal laser scanning microscope (Zeiss LSM 510 Meta, Germany) with argon laser excitation at 488 and 514 nm, autofluorescence with 650 nm emission, and pinholes in 3 airy units.

Cell viability

In order to describe a straightforward methodology to evaluate a pre-treatment technique for the release of *T. obliquus* BR003 metabolites, three samples of viable cultures were washed twice with PBS (0.1 M and pH 7.2) containing 1% (v/v) Triton X-100 by centrifugation (Eppendorf, 5430, Germany) at 4.000 *g* for 5 min and subsequent sonication (Vibra Cell, Sonics and Materials, Inc., USA) for 30 min. The working cycles were 5 s for sonication and 2 s for pulsation, with an amplitude of 40% and frequency of 40 kHz at 50 °C. Finally, the samples were cooled in an ice bath to 25 °C and centrifuged at 4000 *g* for 5 min, followed by incubation with fluorescent markers and photography under the same conditions as conventional confocal microscopy. Intact cells appeared red, while dead or damaged cells were stained green and/or magenta.

Scanning electron microscopy

T. obliquus BR003 cells were fixed in a 2.5% solution (v/v) of glutaraldehyde in 0.05 M sodium cacodylate buffer at pH 7.2 (buffer B) for 2 h and then fixed with a 1% osmium tetroxide solution (m/v) in buffer B at room temperature for 2 h. The cells were washed three times in buffer B, dehydrated in a series of ethanol solutions (70, 80, 90, 95% v/v), and three times in anhydrous ethanol (Ribeiro et al. 2018). The dehydrated cells were dried in hexamethyldisilazane (HMDS), covered with gold (15 nm thick) (Quorum, Q150RS, UK) (Berger et al. 2016), and analyzed under an LEO 1430 VP scanning electron microscope (Carl Zeiss, UK) at 20 kV.

Energy dispersion X-ray spectroscopy

The lyophilized biomass of *T. obliquus* BR003 was covered with carbon (15 nm thick) in an evaporator (Quorum Q150T-E, United Kingdom) to evaluate the distribution of chemical

elements. Next, the system was analyzed in an X-ray microprobe (X-EDS, IXRF Systems, USA) coupled to the LEO 1430 VP scanning electron microscope (Carl Zeiss, UK). The distribution of chemical elements was normalized to the carbon, oxygen, and nitrogen distributions (Ladeira et al. 2020).

Transmission electron microscopy (TEM)

T. obliquus BR003 cells were transferred to a solution at 2.5% (v/v) glutaraldehyde in 0.1 M sodium cacodylate buffer at pH 7.2 (buffer C) containing 2% (m/v) sucrose for 24 h. After this period, the samples were washed with buffer C three times for 10 min. The samples were postfixed in 1% (m/v) osmium tetroxide for 2 h, washed three times with deionized water, dehydrated using a gradient of an aqueous ethanol solution (70, 80, 90, and 95% v/v), and soaked in LR-White resin (London Resin Company, Basingstoke, UK) (Farder-Gomes et al. 2019). Ultrafine sections were arranged in copper grids, contrasted with 5% aqueous solution (m/v) of aqueous uranyl acetate for 30 min, with lead citrate (Reynolds, 1963) for 5 min, and analyzed in a Zeiss Libra 120 transmission electron microscope (Carl Zeiss, Germany).

Results

Biochemistry

In the *T. obliquus* BR003 dry biomass, we identified 61.6% unsaturated fatty acids (UFAs) and 3.4% saturated fatty acids (SFAs). Palmitic acid C16:0 was the main saturated fatty acid (SFA). For monounsaturated fatty acids (MUFAs), oleic acid C18:1n9c was extracted at a higher quantity than elaidic acid C18:1n9t. For polyunsaturated fatty acids (PUFAs), γ-linolenic acid C18:3n6 was obtained in higher quantity than linoleic acid C:18:2n6c. The PUFA/SFA and MUFA/SFA ratios were 0.56 and 1.04, respectively. Regarding other compounds, 28.50 ± 1.47 g soluble proteins/100 g, 0.14 ± 0.009 g carotenoids/100 g, 0.76 ± 0.013 g chlorophyll a/100 g, and 0.42 ± 0.015 g chlorophyll b/100 g with a chlorophyll a/b ratio of 1.8 were detected.

Morphology

The isolated or aggregated cells of *T. obliquus* BR003 were similar, and the following morphological description refers to both types. The cells were elliptical, approximately 10 µm long, individualized (Fig. 1A) or in coenobia of four (Fig. 1B) to eight laterally connected cells (Fig. 1C), but without alignment of the edges (Fig. 1B-C). The cell surface was rough and had longitudinal protrusions in the median region (Fig. 1A).

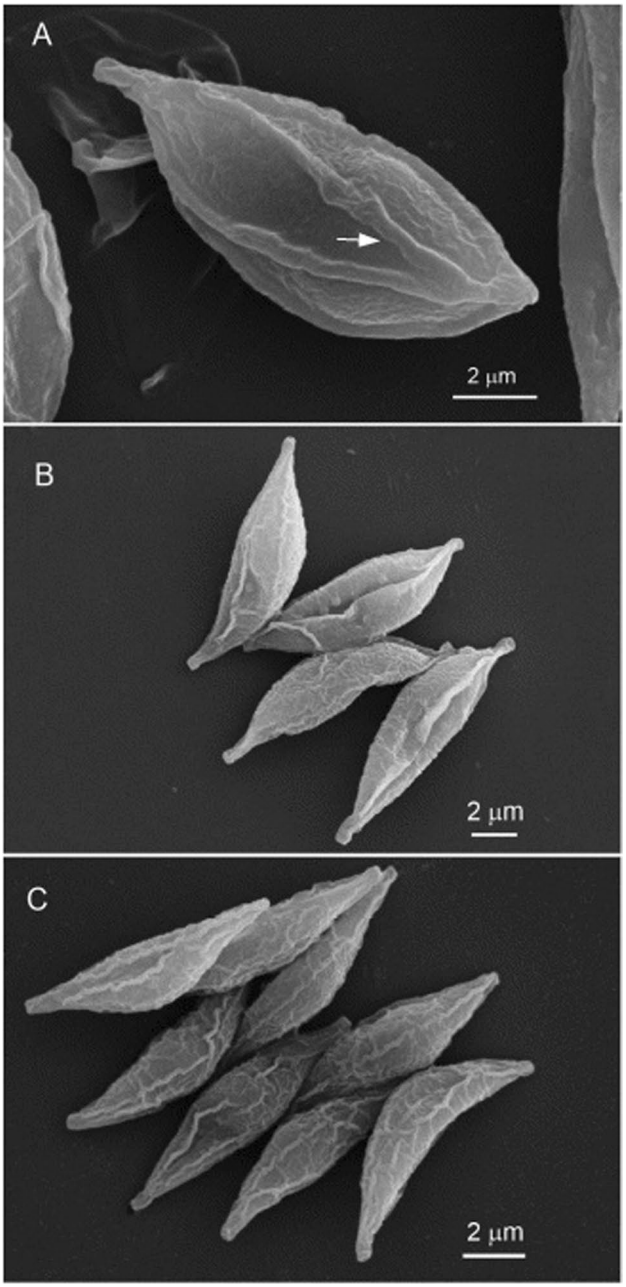

Fig. 1 Scanning electron micrographs of *Tetradesmus obliquus* BR003, showing the cell individualized (**A**) or grouped in coenobia of 4 (**B**) or 8 cells (**C**). Arrow indicates longitudinal ridges

Energy-dispersive X-ray spectroscopy, after normalized by the distribution of carbon, oxygen, and nitrogen, showed that S > Mg > P were the main chemical elements, followed by Co > Zn > Cu, with Mn, Mo, and Si being the most variable (Fig. 2).

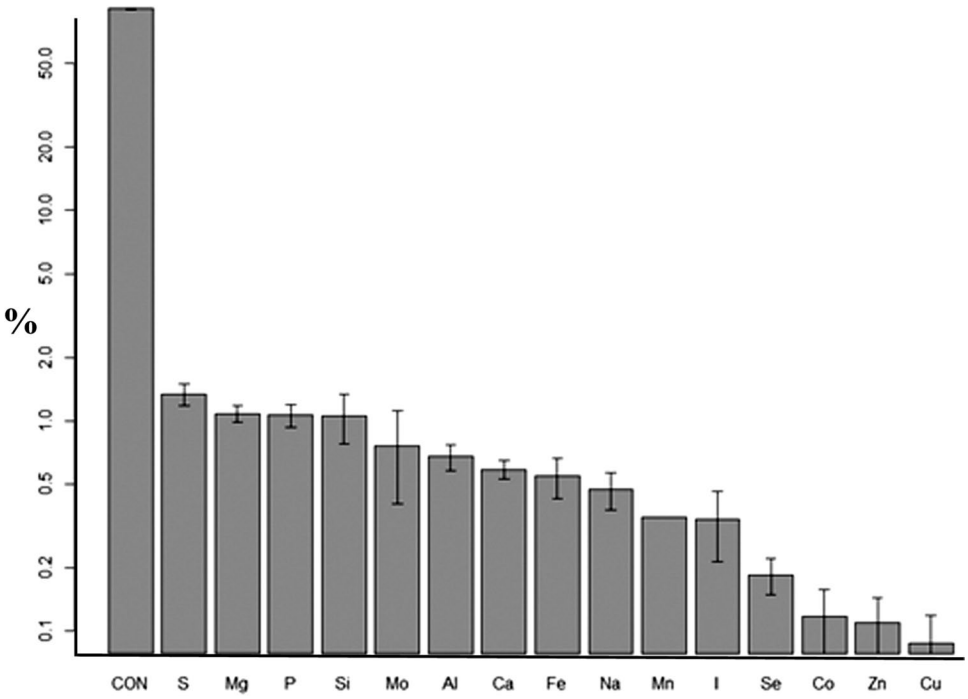

Fig. 2 Percentage distribution (mean ± SD) of chemical elements present in the biomass of *Tetradesmus obliquus* BR003 from energy-dispersive X-ray spectroscopy analysis. The values represent the X-ray emission spectrum for the analyzed elements (X-ray emission spectrum of the element/X-ray emission spectrum of the total elements). CON = sum of the percentages of the elements carbon, oxygen, and nitrogen

Confocal microscopy of intact *T. obliquus cells* showed no positive reaction for proteins (Fig. 3B) and DNA (Fig. 3C), but autofluorescence of chlorophyll was observed (Fig. 3D). However, after treatment with detergent Triton X-100 and mechanical rupture by ultrasound, the autofluorescence remained less expressive (Fig. 3I). There was a positive reaction of proteins (Fig. 3G) and DNA (Fig. 3H). The labeling of protein with fluorescein isothiocyanate was visible and intensified, internalized (empty arrow), and extravasated (double arrow). The labeling of nucleic acids (solid arrow) by propidium iodide was also visible.

Histochemical tests of *T. obliquus* BR003 showed few acidophilic cytoplasmic compartments, some basophilic ones, and basophilic spherical nuclei (Fig. 4A). The PAS test revealed carbohydrates distributed throughout the cytoplasm and a strong reaction in a spherical body in each chloroplast, corresponding to the pyrenoid (Fig. 4B). Histochemistry for lipids indicated some droplets distributed within the cytoplasm (Fig. 4C). The mercury-bromophenol test for total proteins demonstrated a strong positive reaction in the nucleus and cytoplasmic regions (Fig. 4D).

The cells had a well-developed nucleus with some vacuoles, chloroplasts occupying almost the whole cytoplasm, and the predominance of decondensed chromatin (Fig. 5). The cell wall had three well-defined layers (Fig. 6). The outer layer is the trilaminar sheath, followed by a fibrous layer and an electron-dense inner layer in contact with the cell's plasma membrane (Fig. 6A). The cell wall filled the edges of the microalgae with a predominance of fibrous material (Fig. 6B).

Chloroplasts were rich in starch granules, and some were associated with the spherical central pyrenoid (Fig. 7A-C). Starch granules had a crescent moon shape when associated with the pyrenoid. There was an extensive thylakoid membrane that, in some regions, was close to the plastoglobules (Fig. 7C-D). The cytoplasm around the chloroplasts was rich in vacuoles, rough endoplasmic reticulum, mitochondria (Fig. 7B-D), some elements of the Golgi complex (Fig. 8A), and chloroplasts with abundant starch (Fig. 8B). Thus, chloroplasts found in the cytoplasms were starch stores (Fig. 8B).

Discussion

The microalga *Tetradesmus obliquus* BR003, under salt stress conditions, accumulated more esterifiable neutral lipids (mono-, di-, and tri-glycerols) and free fatty acids (Rocha et al. 2019), showing that nutrition and light availability affect the content of important compounds for the bioenergy and food industries. The unsaturated fatty acids of *T. obliquus* BR003 are mostly oleic acid (C18:1n9c) and γ-linolenic acid (C18:3n6), whereas palmitic acid (C16:0) is the main saturated fatty acid (Table 1). The PUFA/SFA (0.56) and MUFA/SFA (1.04) ratios are higher than the minimum recommendation PUFA/SFA of 0.45 for the human diet (Cuthbertson 1989). Fatty acids synthesized by microalgae produced under different growth conditions have 16 to 18 carbons and are similar to the fatty acids found in vascular plants (Guedes et al. 2011; Talebi et al. 2013). Some fatty acids, as palmitic, stearic, elaidic, oleic, linoleic, and

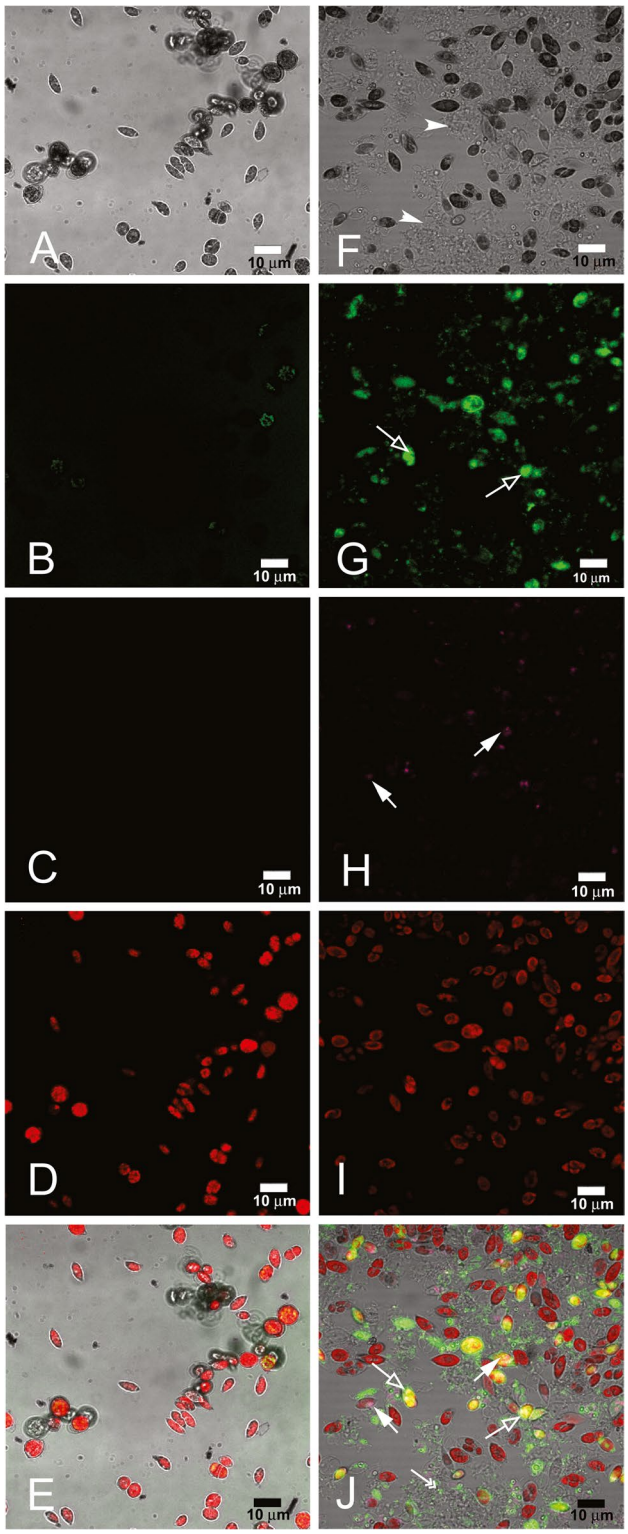

Fig. 3 Confocal microscopy of *Tetradesmus obliquus* BR003. Bright field (**A** and **F**), protein (**B** and **G**) and DNA (**C** and **H**), chlorophyll-autofluorescence (**D** and **I**), and overlap in the microalga control (**E**) and treated with detergent Triton X-100 and subjected to ultrasound rupture (**J**). Empty arrow = intensified internalized protein labeling, double arrow = extravasated protein, solid arrow = nucleic acids

linolenic, are rich in ω-3, ω-6, and ω-9 and can be considered functional and nutraceutical foods. They are also substrates to produce biodiesel. *Arthrospira platensis* (Spirulina) has a PUFA/SFA ratio of 0.88, and this cyanobacterium is a reference for the food industry (Oliveira et al. 2010). Therefore, the fatty acids found in *T. obliquus* BR003 indicate that this microalga has the potential for food application. Some studies have shown that advanced techniques of nutrition and cultivation may stimulate the accumulation of lipids in the *T. obliquus* BR003 strain (Covell et al. 2020; Rocha et al. 2019).

The soluble protein content (28.50 ± 1.47 g soluble/100 g) in *T. obliquus* BR003 is similar to those reported for this species (Rocha et al. 2019). Amorim et al. (2021) shown that in tropical temperatures and under production conditions with an abundance of nitrogen, the strain BR003 is a promising alternative for obtaining biomass rich in protein.

Regarding chlorophyll contents, the total values obtained (1.19 g/100 g) and carotenoids (0.14 g/100 g) are lower than those previously reported for this strain (Covell et al. 2020; Rocha et al. 2017). Chlorophyll a is the most abundant photosynthesizing pigment in *T. obliquus*. The microalgae contain high lutein and chlorophyll b levels than other photosynthesizing pigments like neoxanthin, loroxanthin, and violaxanthin (Wiltshire et al. 2000). Specific cultivation and nutrition procedures can modulate the accumulation of certain biochemical classes (lipids, carbohydrates, or proteins) in *T. obliquus* (Amorim et al. 2020b; Covell et al. 2020; Rocha et al. 2019, 2017; Soares et al. 2018). However, the duration of cultivation of *T. obliquus* BR003 evaluated here was shorter than those in previous studies (Covell et al. 2020; Rocha et al. 2019), which may explain the lower values of some biocompounds.

As for morphology, one of the ornamental characteristics that help identify the genus *Tetradesmus* is the long and curved spines attached to the ends of the cells, as described in two species of *Scenedesmus* by Staehelin and Pickett-Heaps (1975). The present study identified the BR003 strain described in a previous report of molecular phylogeny analyses (Rocha et al. 2017). The use of scanning electron microscopy (Fig. 1) shows us that *T. obliquus* cells are elliptical, without appendages (spines) (Lürling 2003) and curved edges (Hegewald et al. 2013). The genus *Tetradesmus* can form cenobium obes containing 4, 8, 16, or more cells (Giraldo-Zuluaga et al. 2018). We found *T. obliquus* BR003 forming the coenobium obes with eight cells. In Fig. 1A, the BR003 strain presented bulges in the cell length direction that characterize well-defined longitudinal streaks, similar to those observed for two species of non-verrucous *Scenedesmaceae* from a temperate climate. The scanning microscopy also showed the formation of a characteristic coenobium (Hegewald et al., 2013), a defense strategy characteristic of the species (Oliveira et al. 2021).

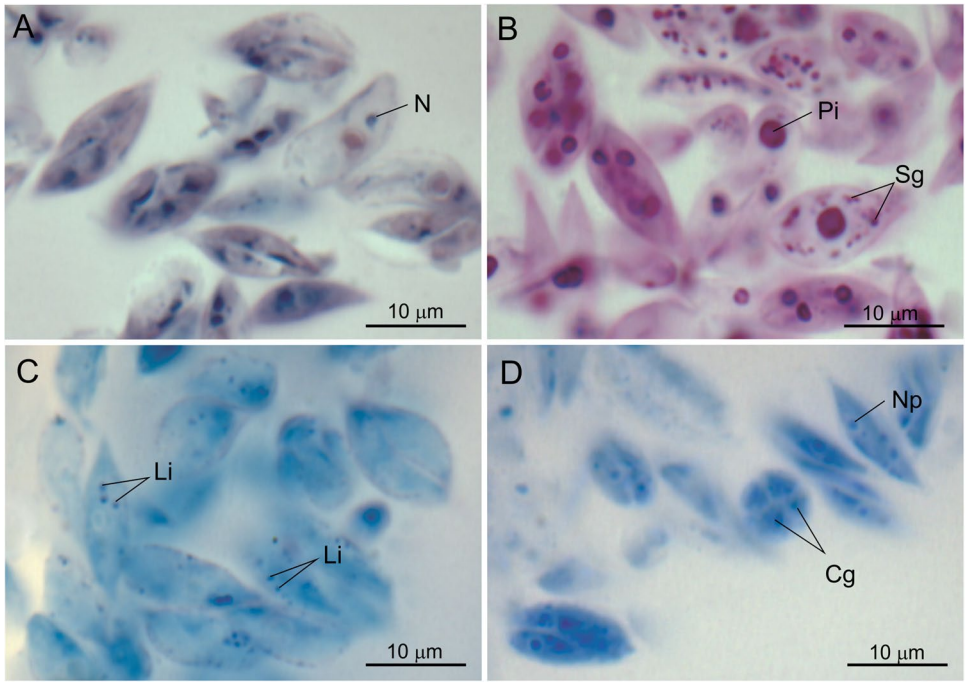

Fig. 4 Histochemistry of microalga *Tetradesmus obliquus* BR003. **A** Conventional staining by hemtoxylin and eosin showing cells with a basophilic nucleus—N and slightly acidophilic cytoplasm. **B** Histochemistry for starch showing a large reserve of starch in a spherical pyrenoid—Pi and small reserves of starch granules—Sg distributed by the cytoplasm. **C** The lipid test showing some lipid droplets—Li distributed through the cytoplasm. **D** The protein test showing an accumulation of nuclear proteins—Np, some strongly labeled cytoplasmic granules—Cg, and the cytoplasm weakly labeled by the test

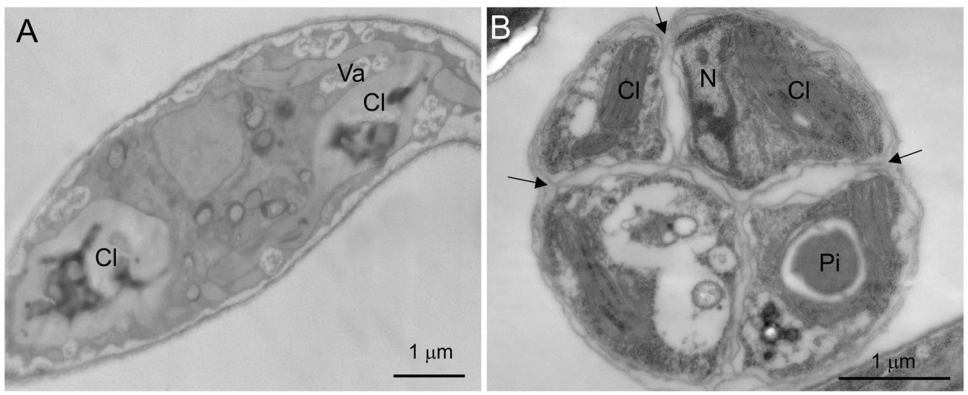

Fig. 5 Transmission electron micrographs of *Tetradesmus obliquus* BR003. **A** Overview of a cell in longitudinal section shown chloroplasts—Cl that occupy most of the cytoplasm and cytoplasmic vacuoles—Va. **B** Cross-section of a group of four cells separated by the cell envelope (arrows). Note that all cells are provided with broad nucleus—N and chloroplasts—Cl containing pyrenoid—Pi

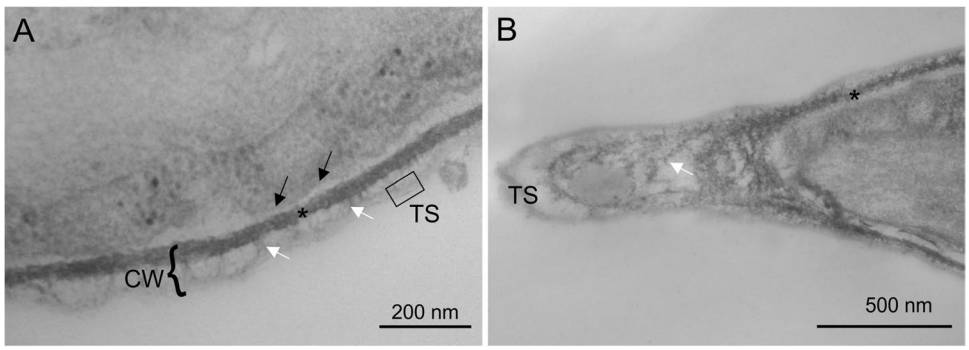

Fig. 6 Transmission electron micrographs of *Tetradesmus obliquus* BR003 showing in detail the cell wall—CW. **A** Three distinct layers form the cell wall; the outermost is the trilaminar sheath—TS, followed by a cellulosic wall layer (fibrous material—white arrows) and the innermost has a higher density mature cell wall (*). The innermost layer is in contact with the cell membrane (black arrows). **B** The ends of the microalgae are filled by the cellulosic wall layer (white arrow). TS = trilaminar sheath; * = mature cell wall layer

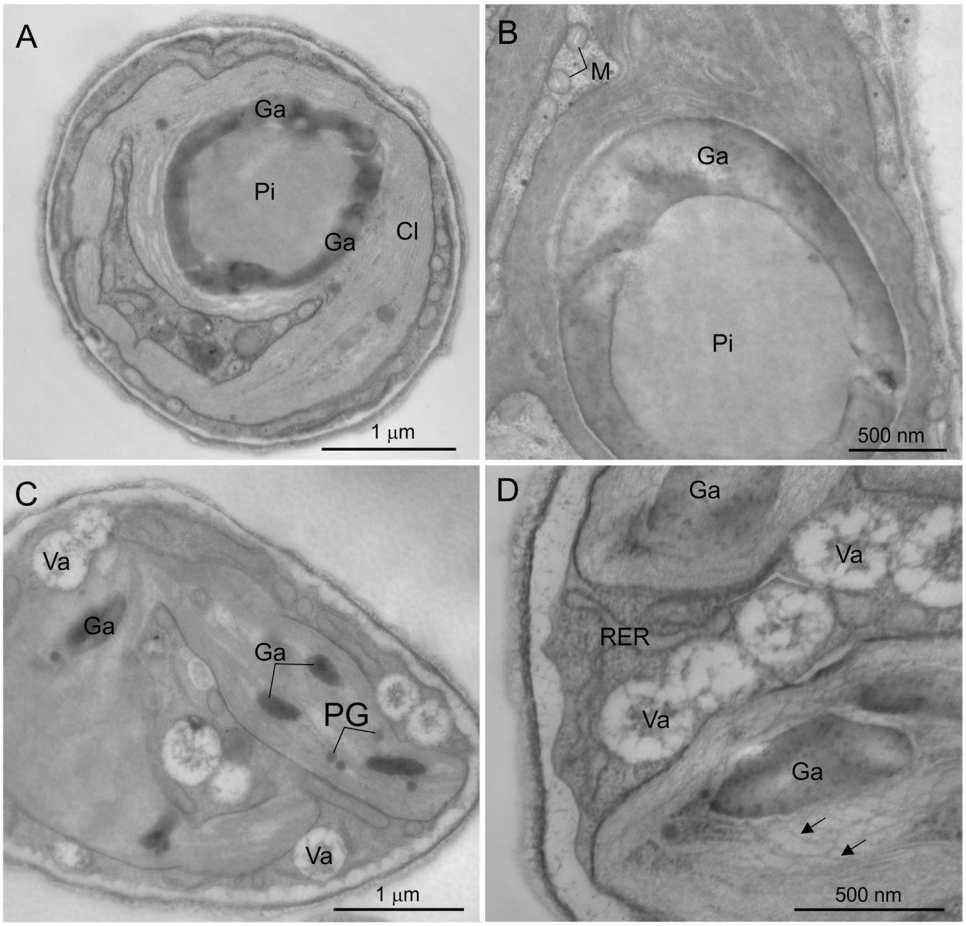

Fig. 7 Transmission electron micrographs of *Tetradesmus obliquus* BR003 showing in detail the chloroplasts. **A** Overview showing that chloroplast—Cl occupies most of the cytoplasm. It has crescent-moon-shaped starch granules—Ga that are associated with a spherical pyrenoid—Pi. **B** Detail of starch grains—Ga surrounding the pyrenoid—Pi. Note the presence of mitochondria—M that are close to the chloroplast. **C** Cross-sectional chloroplast showing the presence of starch grains—Ga and plastoglobules—PG. Note the presence of cytoplasmic vacuoles located around the chloroplasts. **D** Detail of chloroplast showing the organization of thylakoid membranes (black arrows) interspersed with starch granules—Ga. The cytoplasmic region near the chloroplast is rich in rough endoplasmic reticulum—RER. Va = vacuoles

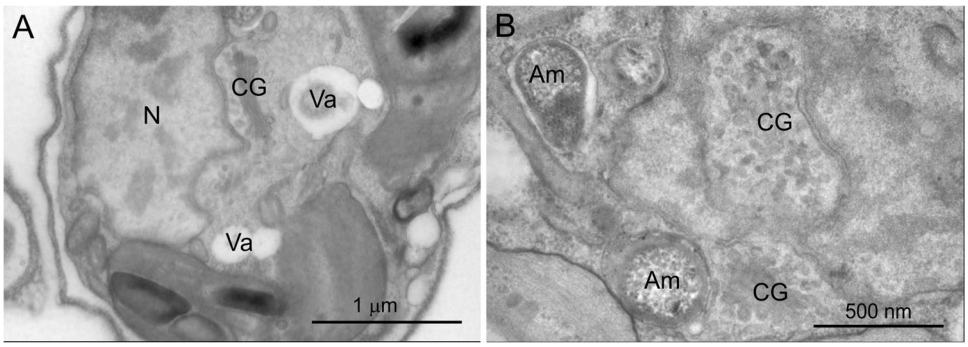

Fig. 8 Transmission electron micrographs of *Tetradesmus obliquus* BR003 showing in detail the cytoplasmic organelles. **A** Nucleus—N formed with decondensed chromatin and some lumps of condensed chromatin. Note element of the Golgi complex—CG and vacuoles—Va. **B** Details of the elements of the Golgi complex—CG in different planes of section and chloroplasts with abundant starch—Am

In the present report, X-ray emission spectra were used to study the chemical composition of *T. obliquus*. Among the chemical elements present in the biomass of *T. obliquus* BR003, we found the element sulfur (S) as the main component, which is poorly studied for microalgal nutrition compared to C, N, and P (Omta et al. 2020; Pedruzi et al. 2020). The elementary distribution also demonstrated that S, Mg, and P are, in this order, the main minerals present in *T. obliquus* BR003, while Co, Zn, and Cu occur in small amounts. Phosphorus and S are some main nutrients for microalgae growth and Fe and Mn in smaller quantities. Co, Zn, and Mo are essential nutrients in very low concentrations (Ghafari et al. 2018).

Table 1 Fatty acids of *Tetradesmus obliquus* BR003 derivatized in HCl/methanol. *nd* not detected

Fatty acids	mg/g	(%)
Palmitic C16:0	11.29	38.4
Stearic C18:0	nd	nd
Elaidic C18:1n9t	3.46	11.8
Oleic C18:1n9c	8.31	28.3
Linoleic C18:2n6c	0.8	2.7
γ-linolenic C: 18:3n6	5.55	18.9
Nervonic C: 24:1	nd	nd
Total	29.41	100
Saturated (SFA)	11.29	38.4
Unsaturated (UFA)	18.12	61.6
Monounsaturated (MUFA)	11.77	40.0
Polyunsaturated (PUFA)	6.35	21.6
PUFA/SFA	0.56	-
MUFA/SFA	1.04	-

A challenge to refine microalgae biomass lies in cell disruption to recover intracellular compounds like lipids and proteins (Amorim et al. 2020a). Thus, the cell wall is the main structure avoiding microalgae cell disruption (Safi et al. 2013), making it necessary pre-treatments to obtain a large compound yield (Khoo et al. 2020; Samarasinghe et al. 2012).

According to the taxonomic classes, the cell wall structures of microalgae differ in their organic constitution (Ryckebosch et al. 2012). In *Phaeodactylum tricornutum* (Bacillariophyceae), for example, different physical and mechanical treatments of cell disruption result in no significant difference in the fatty acid content (Ryckebosch et al. 2012). The cell wall structure of *Tetradesmus* sp. (Chlorophyceae) consists of a rigid carbohydrate network containing glucosamine (aminosaccharide), galactose, mannose, and a higher amount of glucose (Takeda 1996).

In our studies, the protection system of viable cells guaranteed impermeability for the tested fluorochromes (Fig. 3B and 3C), notably for propidium iodide (PI), widely used for bacterial viability assessment, because it stains DNA and RNA inside cells; however, it only crosses compromised plasma membranes and is therefore considered an indicator of cell membrane integrity (Rosenberg et al. 2019). Therefore, when this protective system is sensitized or even partially destroyed, PI can cross the barriers (cell wall, plasma membrane, and nuclear membrane) binding to the DNA. It is still possible to observe in Fig. 3F and Fig. 3J extravasated intracellular content, not seen in Fig. 3A and Fig. 3E. Another observation refers to autofluorescence, and low autofluorescence levels were observed (Fig. 3I) compared to viable cells (Fig. 3D), possibly due to the loss of fluorescent pigments during the applied treatment. Thus, specific pre-treatments are needed for this species to disturb the system, exposing its internal components (Fig. 3J) of great commercial interest (Amorim et al. 2021; Vieira et al. 2021). Therefore, knowing that it is necessary to cause cell disruption to obtain biocompounds (Amorim et al. 2020b), models that allow us to assess the extent of this damage, even if qualitatively, are interesting to propagate. In that regard, we demonstrate that confocal microscopy can be a suitable model to assess pre-treatment techniques for the effective release of microalgal metabolites since intact cells have a good system of protection to external components, unlike injured or damaged cells. Furthermore, the fluorescence of biomarkers can facilitate the visualization or even confirm the extravasation of biocompounds. The confocal microscopy has been used to demonstrate cell damage in terrestrial and aquatic green algae, submitted to water stress with specific labeling for the plasma membrane showing that the dye bound to intracellular content only in cells damaged by desiccation (Cardon et al. 2018; Terlova et al. 2021) such as we found in *T. obliquus* BR003.

The cell wall of *T. obliquus* comprises hydrated silicon dioxide (Navarro et al. 2008), is semipermeable, and provides a protective physical barrier system (Wei et al. 2010). The cell wall has three well-defined layers with cellulose in the inner wall layer, lipids and insoluble glycoproteins, and biopolymers in the trilaminar outer layers that further contribute to the rigidity of this structure (Voigt et al. 2014). The cell wall contains glucose and other neutral sugars such as mannose, fructose, and rhamnose (Blumreisinger et al. 1983; Oliveira et al. 2021). One of the first studies on the *Tetradesmus* ultrastructure, formely *Scenedesmus*, describes cells with a thick cell wall, covered by a trilaminar sheath that presents a warty structure that contributes to cell adhesion and formation of the cenobium (Staehelin and Pickett-Heaps, 1975).

The combined use of carbohydrate test (PAS) and transmission electron microscopy demonstrate chloroplasts with abundant starch as the main carbohydrate reserve structure. However, there are also free carbohydrates in the cytoplasm, which may be associated with metabolic activity and cellular homeostasis maintenance. The pyrenoid matrix strongly reacts to carbohydrates, indicating that a starch sheath covered it (Wang and Jonikas 2020). The starch content is a fraction of the total neutral carbohydrates of *T. obliquus* BR003 (Rocha et al. 2017). Interestingly, the lipid test indicates this component in the cytoplasm, reported in chloroplasts (differentiated plastoglobules) of *Chlamydomonas* strains (Moriyama et al. 2018). The mercury-bromophenol test showed proteins in the nucleus and dispersed in the cytoplasm, corroborating that microalgae do not accumulate proteins in vacuoles (Shebanova et al. 2017). Therefore, the present cytochemical study of *T. obliquus* BR003 demonstrates the intracellular localization of these compounds with potential commercial use.

The occurrence of many chloroplasts with starch granules associated with a central pyrenoid reveals that *T. obliquus* has high photosynthetic activity and energy stock capacity as starch and lipids. Interestingly, starch granules associated with pyrenoids have a crescent moon shape. Pyrenoids are a protein structure that optimizes CO_2 fixation due to the formation of a dense matrix with the enzyme ribulose 1,5-bisphosphate carboxylase/oxygenase (RuBisCO) (Wang and Jonikas 2020). The chloroplasts observed here are rich in thylakoid membranes that, in some regions, have plastoglobules that can perform the lipid reserve function, as reported in other algae (Moriyama et al. 2018). Our findings are similar to reported for another strain of *T. obliquus* with a single cup-shaped chloroplast with a pyrenoid surrounded by several starch grains of different sizes (Terlova et al. 2021).

The cells of *T. obliquus* have many free ribosomes, well-developed rough endoplasmic reticulum, and Golgi complex, indicating high protein synthesis. These proteins can be stored as reported for *A. platensis* (Spirulina), cyanobacteria commercially cultivated to produce dietary supplements (Amorim et al. 2020a, b; Silva et al. 2020; Soares et al. 2018).

The cells of *T. obliquus* BR003 evaluated here did not have high levels of carbon reserve structures, such as starch and lipids, probably because they were neither sampled in the stationary growth phase nor cultivated under stress conditions (Rocha et al. 2019; Soares et al. 2018). These microalgae may store 38% starch (Breuer et al. 2014) and 45% triacylglycerols (Jaeger 2014).

Plastoglobules from green algae and higher plants are lipophilic droplets adhered to the thylakoid membranes of chloroplasts (Lohscheider and Río Bártulos 2016). The finding of lipid droplets dispersed in the cytoplasm of this species shows a diversified distribution of fat-soluble components in the cell. This study also shows that *T. obliquus* BR003 has several starch granules and few lipid bodies, which strongly suggests that these microalgae can be cultivated to produce carbohydrates. Also, this study is innovative because it uses the X-ray emission spectrum in *T. obliquus* and found that S is the main macronutrient.

Acknowledgements The authors thank the Nucleus of Microscopy and Microanalysis of UFV for technical assistance.

Funding This study was financially supported by the PETROBRAS (Petróleo Brasileiro), the Minas Gerais State Research Support Foundation (FAPEMIG), the National Council for Scientific and Technological Development (CNPq), and the Coordination for the Improvement of Higher Education Personnel (CAPES).

Declarations

Conflict of interest The authors declare no competing interests.

References

Amorim ML, Soares J, dos Coimbra JS, R, Leite M de O, Albino LFT, Martins MA, (2020a) Microalgae proteins: production, separation, isolation, quantification, and application in food and feed. Crit Rev Food Sci Nutr 61:1–27. https://doi.org/10.1080/10408398.2020.1768046

Amorim ML, Soares J, Vieira BB, Batista-Silva W, Martins MA (2020b). Extraction of proteins from the microalga Scendesmus obliquus BR003 followed by lipid extraction of the wet deproteinized biomass using hexane and ethyl acetate. Bioresour Technol 307https://doi.org/10.1016/j.biortech.2020.123190

Amorim ML, Soares J, Vieira BB, de Leite M, O, Rocha DN, Eleuterio P, (2021) Pilot-scale biorefining of the microalga Scenedesmus obliquus for the production of crude lipids and protein concentrate. Sep Purif Technol 270:1–9. https://doi.org/10.1016/j.seppur.2021.118775

Barkallah M, Dammak M, Louati I, Hentati F, Hadrich B, Mechichi T, Ayadi MA, Fendri I, Attia H, Abdelkafi S (2017) Effect of Spirulina platensis fortification on physicochemical, textural, antioxidant and sensory properties of yogurt during fermentation and storage. LWT- Food Sci Technol 84:323–330. https://doi.org/10.1016/j.lwt.2017.05.071

Bensalem S, Pareau D, Cinquin B, Français O, Pioufle BL, Lopes F (2020) Impact of pulsed electric fields and mechanical compressions on the permeability and structure of Chlamydomonas reinhardtii cells. Sci Rep 10:1–11. https://doi.org/10.1038/s41598-020-59404-6

Berger LRR, Stamford NP, Willadino LG, Laranjeira D, de Lima MAB, Malheiros SMM, Stamford TCM (2016) Cowpea resistance induced against Fusarium oxysporum f. sp. tracheiphilum by crustaceous chitosan and by biomass and chitosan obtained from Cunninghamella elegans. Biol Control 92:45–54. https://doi.org/10.1016/j.biocontrol.2015.09.006

Bermejo R, Ruiz E, Acien FG (2007) Recovery of B-phycoerythrin using expanded bed adsorption chromatography: scale-up of the process. Enzyme Microb Technol 40:927–933. https://doi.org/10.1016/j.enzmictec.2006.07.027

Blumreisinger M, Meindl D, Loos E (1983) Cell wall composition of chlorococcal algae. Phytochemistry 22(7):1603–1604. https://doi.org/10.1016/0031-9422(83)80096-x

Breuer G, de Jaeger L, Artus VPG, Martens DE, Springer J, Draaisma RB, Eggink G, Wijffels RH, Lamers PP (2014) Superior triacylglycerol (TAG) accumulation in starchless mutants of Scenedesmus obliquus: (II) evaluation of TAG yield and productivity in controlled photobioreactors. Biotechnol Biofuels 7:1–11. https://doi.org/10.1186/1754-6834-7-70

Cardon ZG, Peredo EL, Dohnalkova AC, Gershone HL, Bezanilla M (2018) A model suite of green algae within the Scenedesmaceae for investigating contrasting desiccation tolerance and morphology. J Cell Sci 131:1–11. https://doi.org/10.1242/jcs.212233

de Castro MBA, Martinez LC, Cossolin JFS, Serra RS, Serrão JE (2020) Cytotoxic effects on the midgut, hypopharyngeal, glands and brain of Apis mellifera honey bee workers exposed to chronic concentrations of lambda-cyhalothrin. Chemosphere 248:1–11. https://doi.org/10.1016/j.chemosphere.2020.126075

Covell L, Machado M, Vaz MGMV, Soares J, Batista AD, Araújo WL, Martins MA, Nunes-Nesi A (2020) Alternative fertilizer-based growth media support high lipid contents without growth impairment in Scenedesmus obliquus BR003. Bioprocess Biosyst Eng 43:1123–1131. https://doi.org/10.1007/s00449-020-02301-z

Cuthbertson WFJ (1989) What is a healthy food? Food Chem 33:53–80. https://doi.org/10.1016/0308-8146(89)90100-3

Dahlin LR, Van Wychen S, Gerken HG, McGowen J, Pienkos PT, Posewitz MC, Guarnieri MT (2018) Down-selection and

outdoor evaluation of novel, halotolerant algal strains for winter cultivation. Front Plant Sci 9:1–10. https://doi.org/10.3389/fpls.2018.01513

Falconí JHH, Soares J, Rocha DN, Vaz MGMV, Martins MA (2021) Strain screening and ozone pretreatment for algae farming in wastewaters from sugarcane ethanol biorefinery. J Clean Prod 282:1–10. https://doi.org/10.1016/j.jclepro.2020.124522

Farder-Gomes CF, Santos HCP, Oliveira MA, Zanuncio JC, Serrão JE (2019) Morphology of ovary and spermathecae of the parasitoid Eibesfeldtphora tonhascai Brown (Diptera: Phoridae). Protoplasma 256:3–11. https://doi.org/10.1007/s00709-018-1276-3

Fradique M, Batista AP, Nunes MC, Gouveia L, Bandarra NM, Raymundo A (2010) Incorporation of Chlorella vulgaris and Spirulina maxima biomass in pasta products. Part 1: preparation and evaluation. J Sci Food Agric 90:1656–1664. https://doi.org/10.1002/jsfa.3999

García-Segovia P, Pagán-Moreno MJ, Lara IF, Martínez-Monzó J (2017) Effect of microalgae incorporation on physicochemical and textural properties in wheat bread formulation. Food Sci Technol Int 23:437–447. https://doi.org/10.1177/1082013217700259

Ghafari M, Rashidi B, Haznedaroglu BZ (2018) Effects of macro and micronutrients on neutral lipid accumulation in oleaginous microalgae. Biofuels 9:147–156. https://doi.org/10.1080/17597269.2016.1221644

Giraldo-Zuluaga J-H, Salazar A, Diez G, Gomez A, Martínez T, Vargas JF, Peñuela M (2018) Automatic identification of Scenedesmus polymorphic microalgae from microscopic images. Pattern Anal Appl 21:601–612. https://doi.org/10.1007/s10044-017-0662-3

Guedes AC, Amaro HM, Barbosa CR, Pereira RD, Malcara FX (2011) Fatty acid composition of several wild microalgae and cyanobacteria, with a focus on eicosapentaenoic, docosahexaenoic and α-linolenic acids for eventual dietary uses. Food Res Int 44:2721–2729. https://doi.org/10.1016/j.foodres.2011.05.020

Hegewald E, Bock C, Krienitz L (2013) A phylogenetic study on Scenedesmaceae with the description of a new species of Pectinodesmus and the new genera Verrucodesmus and Chodatodesmus (Chlorophyta, Chlorophyceae). Fottea 13:149–164. https://doi.org/10.5507/fot.2013.013

Hossain AKMM, Brennan MA, Mason SL, Guo X, Zeng XA, Brennan CS (2017) The effect of astaxanthin-rich microalgae "Haematococcus pluvialis" and wholemeal flours incorporation in improving the physical and functional properties of cookies. Foods 6:1–10. https://doi.org/10.3390/foods6080057

Ichihara K, Fukubayashi Y (2010) Preparation of fatty acid methyl esters for gas-liquid chromatography. J Lipid Res 51:635–640. https://doi.org/10.1194/jlr.D001065

Khoo KS, Chew KW, Yew GY, Leong WH, Chai YH, Show PL, Chen WH (2020) Recent advances in downstream processing of microalgae lipid recovery for biofuel production. Bioresour Technol 304:1–11. https://doi.org/10.1016/j.biortech.2020.122996

Ladeira LCM, dos Santos EC, Valente GE, da Silva J, Santos TA, dos Maldonado IR, SC, (2020) Could biological tissue preservation methods change chemical elements proportion measured by energy dispersive X-ray spectroscopy? Biol Trace Elem Res 196:168–172. https://doi.org/10.1007/s12011-019-01909-x

Lichtenthaler HK (1987) Chlorophylls and carotenoids: pigments of photosynthetic biomembranes. Meth Enzymol 148:350–382. https://doi.org/10.1016/0076-6879(87)48036-1

Lohscheider JN, Río Bártulos C (2016) Plastoglobules in algae: a comprehensive comparative study of the presence of major structural and functional components in complex plastids. Mar Genomics 28:127–136. https://doi.org/10.1016/j.margen.2016.06.005

Lowry OH, Rosebrough NJ, Lewis Farr A, Randall RJ (1951) Protein measurement with the folin Phenol Reagent. J Biol Chem 193:256–275. https://doi.org/10.1016/S0021-9258(19)52451-6

Lürling M (2003) Phenotypic plasticity in the green algae Desmodesmus and Scenedesmus with special reference to the induction of defensive morphology. Ann Limnol - Int J Limnol 39:85–101. https://doi.org/10.1051/limn/2003014

Meijer EA, Wijffels RH (1998) Development of a fast, reproducible and effective method for the extraction and quantification of proteins of micro-algae. Biotechnol Tech 12:353–358. https://doi.org/10.1023/A:1008814128995

Moriyama T, Toyoshima M, Saito M, Wada H, Sato N (2018) Revisiting the algal "chloroplast lipid droplet": the absence of an entity that is unlikely to exist. Plant Physiol 176:1519–1530. https://doi.org/10.1104/pp.17.01512

Navarro E, Baun A, Behra R, Hartmann NB, Filser J, Ai-Jun M, Quigg A, Santschi PH, Sigg L (2008) Environmental behavior and ecotoxicity of engineered nanoparticles to algae, plants, and fungi. Ecotoxicology 17:372–386. https://doi.org/10.1007/s10646-008-0214-0

Oliveira CYB, Oliveira CDL, Pradad R, Ong HC, Araujo ES, Shabnam N, Gálvez AO (2021) A multidisciplinary review of Tetradesmus obliquus: a microalga suitable for large-scale biomass production and emerging environmental applications. Rev Aquac 13:1–25. https://doi.org/10.1111/raq.12536

Oliveira EG, Duarte JH, Moraes K, Crexi VT, Pinto LAA (2010) Optimisation of Spirulina platensis convective drying: evaluation of phycocyanin loss and lipid oxidation. Int J Food Sci Technol 45:1572–1578. https://doi.org/10.1111/j.1365-2621.2010.02299.x

Omta AW, Talmy D, Inomura K, Irwin A, Finkel Z, Sher D, Liefer J, Follows M (2020) Quantifying nutrient throughput and DOM production by algae in continuous culture. J Theor Biol 494:1–12. https://doi.org/10.1016/j.jtbi.2020.110214

Pearse AGE (1953) Histochemistry: theoretical and applied. [s.l.] Little, Brown & Company

Pedruzi GOL, Amorim ML, Santos RR, Martins MA, Vaz MGMV (2020) Biomass accumulation-influencing factors in microalgae farms. Rev Bras Eng Agric e Ambient 24:134–139. https://doi.org/10.1590/1807-1929/agriambi.v24n2p134-139

Reynolds ES (1963) The use of lead citrate at high pH as an eletron-opaque stain in electron microscopy. J Cell Biol 17:208–212. https://doi.org/10.1083/jcb.17.1.208

Ribeiro KVG, Ribeiro C, Dias RS, Cardoso SA, de Paula SO, Zanuncio JC, de Oliveira LL (2018) Bacteriophage isolated from sewage eliminates and prevents the establishment of Escherichia coli biofilm. Adv Pharm Bull 8:85–95. https://doi.org/10.15171/apb.2018.011

Rippka R, Deruelles J, Waterbury JB, Herdman M, Stanier RY (1979) Generic assignments, strain histories and properties of pure cultures of cyanobacteria. Microbiology 111:1–61. https://doi.org/10.1099/00221287-111-1-1

Rizwan M, Mujtaba G, Memon SA, Kisay L, Naim R (2018) Exploring the potential of microalgae for new biotechnology applications and beyond: a review. Renew Sustain Energy Rev 92:394–404. https://doi.org/10.1016/j.rser.2018.04.034

Rocha DN, Martins MA, Soares J, Vaz MGMV, de Leite M, O, Covell L, Mendes LBB, (2019) Combination of trace elements and salt stress in different cultivation modes improves the lipid productivity of *Scenedesmus* spp. Bioresour Technol 289:1–10. https://doi.org/10.1016/j.biortech.2019.121644

Rocha RP, Machado M, Vaz MGMV, Vinson C, Leite MO, Richard R, Mendes L, Araujo W, Caldana C, Martins M, Williams T, Less N-N (2017) Exploring the metabolic and physiological diversity of native microalgal strains (Chlorophyta) isolated from tropical freshwater reservoirs. Algal Res 28:139–150. https://doi.org/10.1016/j.algal.2017.10.021

Rosenberg M, Azevedo NF, Ivask A (2019) Propidium iodide staining underestimates viability of adherent bacterial cells. Sci Report 9:1–12. https://doi.org/10.1038/s41598-019-42906-3

Rubio-Rodríguez N, Beltrán S, Jaime I, de Diego M, Sanz MT, Carballido JR (2010) Production of omega-3 polyunsaturated fatty acid concentrates: a review. Innov Food Sci Emerg Technol 11:1–12. https://doi.org/10.1016/j.ifset.2009.10.006

Ryckebosch E, Muylaert K, Foubert I (2012) Optimization of an analytical procedure for extraction of lipids from microalgae. J Am Oil Chem Soc 89:189–198. https://doi.org/10.1007/s11746-011-1903-z

Safi C, Charton M, Pignolet O, Silvestre F, Vaca-Garcia C, Pontalier P-Y (2013) Influence of microalgae cell wall characteristics on protein extractability and determination of nitrogen-to-protein conversion factors. J Appl Phycol 25:523–529. https://doi.org/10.1007/s10811-012-9886-1

Samarasinghe N, Fernando S, Lacey R, Faulkner WB (2012) Algal cell rupture using high pressure homogenization as a prelude to oil extraction. Renew Energ 48:300–308. https://doi.org/10.1016/j.renene.2012.04.039

Shebanova A, Ismagulova T, Solovchenko A, Baulina O, Lobakova E, Ivanova A, Moiseenko A, Shaitan K, Polshakov V, Nedbal L, Gorelova O (2017) Versatility of the green microalga cell vacuole function as revealed by analytical transmission electron microscopy. Protoplasma 254:1323–1340. https://doi.org/10.1007/s00709-016-1024-5

Silva MET da, Correa K de P, Martins MA, da Matta SLP, Martino HSD, Coimbra JS dos R (2020) Food safety, hypolipidemic and hypoglycemic activities, and in vivo protein quality of microalga *Scenedesmus obliquus* in Wistar rats. J Funct Foods 65:1-12. https://doi.org/10.1016/j.jff.2019.103711

Soares J, Kriiger Loterio R, Rosa RM, Santos MO, Nascimento AG, Santos NT, Williams CR, Nunes-Nesi A, Martins MA (2018) *Scenedesmus* sp. cultivation using commercial-grade ammonium sources. Ann Microbiol 68:35–45. https://doi.org/10.1007/s13213-017-1315-x

Staehelin LA, Pickett-Heaps JD (1975) The ultrastructure of *Scenedesmus* (chlorophyceae). I. Species with the "reticulate" or "warty" type of ornamental layer. J Phycol 11:163–185. https://doi.org/10.1111/j.1529-8817.1975.tb02765.x

Takeda H (1996) Cell wall sugars of some *Scenedesmus* species. Phytochemistry 42:673–675. https://doi.org/10.1016/0031-9422(95)00952-3

Takeshita T, Ota S, Yamazaki T, Hirata A, Zachleder V, Kawano S (2014) Starch and lipid accumulation in eight strains of six Chlorella species under comparatively high light intensity and aeration culture conditions. Bioresour Technol 158:127–134. https://doi.org/10.1016/j.biortech.2014.01.135

Talebi AF, Mohtashami SK, Tabatabaei M, Tohidfar M, Bagheri A, Zeinalabedini M, Mirzaei HH, Mirzajanzadeh M, Shafaroudi SM, Bakhtiari S (2013) Fatty acids profiling: a selective criterion for screening microalgae strains for biodiesel production. Algal Res 2:258–267. https://doi.org/10.1016/j.algal.2013.04.003

Terlova EF, Holzinger A, Lewis AL (2021) Terrestrial green algae show higher tolerance to dehydration than do their aquatic sister-species. Microb Ecol. https://doi.org/10.1007/s00248-020-01679-3

Uribe-Wandurraga ZN, Igual M, García-Segovia P, Martínez-Monzó J (2019) Effect of microalgae addition on mineral content, colour and mechanical properties of breadsticks. Food Funct 10:4685–4692. https://doi.org/10.1039/C9FO00286C

Vieira BB, Soares J, Amorim ML, Bittencourt PVQ, Superbi RC, de Oliveira EB, Coimbra JS dos R, Martins MA (2021) Optimized extraction of neutral carbohydrates, crude lipids and photosynthetic pigments from the wet biomass of the microalga *Scenedesmus obliquus* BR003. Sep Purif Technol 269https://doi.org/10.1016/j.seppur.2021.118711

Voigt J, Stolarczyk A, Zych M, Male P, Burczyk J (2014) The cell-wall glycoproteins of the green alga *Scenedesmus obliquus*. The predominant cell-wall polypeptide of *Scenedesmus obliquus* is related to the cell-wall glycoprotein gp3 of Chlamydomonas reinhardtii. Plant Sci 215–216:39–47. https://doi.org/10.1016/j.plantsci.2013.10.011

Wang L, Jonikas MC (2020) The pyrenoid. Curr Biol 30:456–458. https://doi.org/10.1016/j.cub.2020.02.051

Wei C, Zhang Y, Guo J, Han B, Yang X, Yuan J (2010) Effects of silica nanoparticles on growth and photosynthetic pigment contents of *Scenedesmus obliquus*. J Environ Sci 22:155–160. https://doi.org/10.1016/s1001-0742(09)60087-5

Wiltshire KH, Boersma M, Möller A, Buhtz H (2000) Extraction of pigments and fatty acids from the green alga *Scenedesmus obliquus* (Chlorophyceae). Aquat Ecol 34:119–126. https://doi.org/10.1023/A:1009911418606

Wynne MJ, Hallan JK (2015) Reinstatement of Tetradesmus G. M. Smith (Sphaeropleales, Chlorophyta). Feddes Repert 126:83–86. https://doi.org/10.1002/fedr.201500021